PbS Quantum Dots with Stable Efficient Luminescence in the Near-IR Spectral Range**

By *Ludmila Bakueva*, *Ivan Gorelikov*, *Sergei Musikhin*, *Xu Sheng Zhao*, *Edward H. Sargent*, and *Eugenia Kumacheva**

Rapid progress in tailoring the size and shape of semiconductor nanocrystals (quantum dots) enables a high degree of control over their optical and electronic properties. This control can be harnessed for applications in biological assays, optoelectronic integration, and wireless-systems engineering. In optoelectronics, size tunability of quantum dots permits control over the spectrum of absorption for photovoltaic and photoluminescent, stimulated emission, and electroluminescence applications,[1–4] whereas in biological applications, this allows spectral multiplexing and coding.[5] In both applications, luminescence in the near-infrared region is urgently needed: in optoelectronics to bridge interconnects with short- and medium-haul networks, and in biological applications to exploit the spectral windows in water and biological absorption.

An ideal nanocrystal (NC) synthetic route combines features that have so far been demonstrated in isolation. Synthesis in aqueous solution, or transfer from organic media to water, is highly desirable for compatibility with biological assays.[5] It also enables multilayer polymer–nanocrystal device fabrication for heterostructure engineering through the use of alternating aqueous/organic solvents in sequential layers. Other crucial features of synthetic route are simplicity, use of non-toxic solvents, and moderate reaction temperatures.[6,7] From the point of view of the resulting material properties, the NCs desired in the above-mentioned applications would be size-tunable in the near-IR spectral range; have a high quantum yield, and exhibit stable, narrow fluorescence peaks[8] requiring no yield-reducing size-selective precipitation.
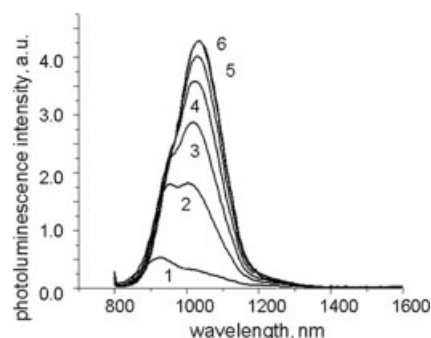
To date, no route to synthesis of quantum dots (QDs) has been reported that accommodates *all* of these features simultaneously. We report herein a one-stage water-based synthesis of stable and monodisperse PbS NCs that show photo- and electroluminescence in the spectral range 1000–1400 nm. It is the *combination* of the simplicity of water-based synthesis, a one-stage process with no need in encapsulation or size-selective precipitation, relatively low toxicity,[9,10] stability, size tunability, and excellent performance that make these NCs promising in optoelectronic and biological applications.

PbS nanocrystals were prepared in aqueous solutions using a mixture of thiols as a stabilizing agent. We admit that water-based synthesis and thiol ligands have been used in II–VI nanoparticle synthesis.[11,12] This approach, however, has not been tested in the preparation of PbS NCs: previous reports on PbS nanoparticles synthesis in aqueous solutions employed poly(vinyl alcohol), poly(vinyl pyrrolidone), gelatin, and DNA as stabilizers.[13,14] These reports and our experiments indicate that these methods result in agglomerates of poly/nanocrystals of very small diameter (~ 1 nm) and absorption and luminescence in the visible spectral range.

We examined a number of different capping agents, such as thiobutanol, thiohexanol, triglycolic acid, thioglycerol, and dithioglycerol. The combination of thioglycerol (TGL) and dithioglycerol (DTG) resulted in nanocrystals of the best quality. In our synthesis, 15 mL of solution containing 2.5×10^{-4} mol of $Pb(CH_3COO)_2$, 1.5×10^{-3} mol of TGL, and 5×10^{-4} mol of DTG was adjusted to pH 11 by addition of triethylamine, and then the solution was cooled to 0 °C using an ice bath.[15] (Cooling was necessary when TGL was used as a sole stabilizer: when a mixture of TGL/DTG was used the synthesis was performed at a room temperature without NC aggregation). A 0.1 M solution of sodium sulfide was then added to the mixture within 1–2 s under vigorous stirring (1250 rpm). The molar ratio Pb/S varied from 1:0.3 to 1:0.7. The color of the resulting solution changed from transparent to dark-brown. The typical concentration of NCs in the solution was ca. 3.2 mg mL^{-1}, however good quality NCs were also prepared at NP concentration as high as 20 mg mL^{-1}.

We studied the variation in NC size after synthesis by examining their time-dependent photoluminescence. Figure 1 shows the time evolution of photoluminescence spectra of the NCs stabilized with TGL–DTG capping ligands. Over time, the shorter-wavelength maximum shrank and ultimately disappeared while the longer-wavelength maximum evolved, increased, and finally stabilized. The intensity of photolumi-

[*] Prof. E. Kumacheva, I. Gorelikov, Dr. X. S. Zhao
Department of Chemistry, University of Toronto
80 Saint George Street, Toronto, OT, M5S 3H6 (Canada)
E-mail: ekumache@chem.utoronto.ca
Dr. L. Bakueva, Dr. S. Musikhin, Prof. E. H. Sargent
Department of Electrical & Computer Engineering
University of Toronto 10 King's College Road
Toronto, OT, M5S 3G4 (Canada)

Figure 1. Time evolution of photoluminescence spectra for aqueous solution of PbS NCs. The curves presented correspond to 0 min (1), 20 min (2), 40 min (3), 60 min (4), 80 min (5), and one month (6). Molar ratio of Pb/TGL/DTG was 1:6:2. Pb/S molar ratio was 1:0.5.

nescence increased during this process and then saturated to a constant level. The ultimate luminescence spectra has a width of ca. 100–150 nm, narrower than 200 nm measured for PbS NCs synthesized in organic solvents[3] and 200–230 nm obtained for HgTe and CdHgTe NCs synthesized in the aqueous medium (for the same spectral range).[16] The photoluminescence spectrum measured a month later did not show any notable change. Since the two luminescence peaks in spectra given in Figure 1 evolved differently in time, we associate these with different fractions of nanoparticles rather than the first and second quantum states of the same NCs. We attribute the redistribution of peak intensities in the first stage of evolution to Ostwald ripening,[17] wherein the growth of the larger particles occurred at the expense of smaller ones, resulting in a decrease in the net surface energy. The size distribution and luminescence characteristics stabilize once the smaller particles are consumed.

When only TGL was used as a stabilizer, the NCs rapidly increased in size and ultimately aggregated, leading to unstable photoluminescence. Similarly, when DTG was used as a sole capping agent the NCs were polydisperse.

The stable behavior of our samples resulted from i) a much stronger bonding of DTG to the NCs surface than that of TGL through the formation of two bonds between DTG and a given Pb atom and ii) a very delicate balance between the amount of DTG and Pb^{2+} ions in solution. As further confirmation, we found that when the molar ratio DTG/Pb^{2+} ions in solution exceeded a value of 3.2, NC formation took up to 10 h (or no PbS crystals would be formed) due to the saturation of Pb^{2+} with ligands, whereas when the above-mentioned ratio was below 1.0, rapid PbS growth and aggregation could not be suppressed.

By varying synthetic conditions, e.g., Pb/S ratio we showed the variation in NC diameter and hence the change in absorption and emission spectra (Figs. 2A,B, respectively). In Figure 2A, a shoulder in the absorption spectra was clearly seen, pointing to the presence of NCs of different sizes. In photoluminescence spectra (Fig. 2B) the emission peak varied from 1000 to 1330 nm, which, according to the theoretical calculations,[18] corresponds to NC diameters from 2.7 to 4.0 nm. The Stokes shift between absorption and photoluminescence maxima increased noticeably from curve 1 to 4, that is with the increase of NC size. This effect was anticipated: large interlevel gaps in small NCs inhibited the energy relaxation process responsible for this shift. Absolute measurements of photoluminescence conducted as described by Friend and co-workers[19] revealed photoluminescence quantum efficiency 17 % for NCs obtained at a molar ratio of Pb/S/DTG/TGL 1:0.5:2:6.

Figure 3A shows typical X-ray diffraction patterns of the powdered NCs stabilized with a mixture of DTG/TGL, taken 1 h (bottom pattern) and 14 days (top pattern) after PbS synthesis. The broadness of the diffraction peaks, especially for the freshly prepared samples, was ascribed to the small size of the PbS NCs.[20] All ten reflections matched well the reference powder diffraction pattern of PbS. The crystal structure de-
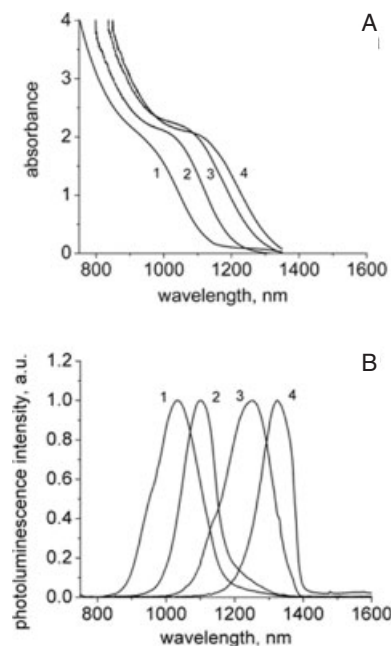

Figure 2. Absorption (A) and photoluminescence (B) spectra for NCs with different sizes, obtained by changing the Pb/S molar ratio: 1) 1:0.3, 2) 1:0.4, 3) 1:0.5, 4) 1:0.7. Molar ratio of Pb/TGL/DTG was 1:6:2. Measurements were taken 3 days after sample preparation.

rived from the positions of the wide-range diffraction peaks clearly indicated a cubic PbS phase. The average crystallite size was measured using direct convolution profile fitting procedure performed by Topas v.2.1.[21] Two other analytical approaches were carried out in order to obtain independently the values for both crystallite size and lattice parameters; that is, the whole powder pattern decomposition and Rietveld refinement. The results of these three methods showed very close values for size of nanocrystals obtained from the ten reflections, yielding 3 nm for the freshly prepared sample NCs and 4 nm for the NCs stored for two weeks. Figure 3B shows a typical transmission electron microscopy (TEM) image of the PbS NCs obtained using an optimized protocol: the nanoparticles remained well separated and the measured NC diameter was 4 ± 1 nm.

We studied the optical properties of PbS NCs in aqueous solution and in conducting polymer–NC composites. First, we used the PbS NCs to fabricate electroluminescent devices.[22] Current–voltage characteristics of the structures exhibited an almost symmetric but strongly nonlinear character consistent with that of known polymer–nanocrystal composites emitting in the visible spectrum.[23]

Figure 4A shows photo- and electroluminescence spectra of the composite structures. Absolute measurements of photoluminescence revealed an external efficiency of 5 %. When we applied a voltage of either polarity exceeding 4–5 V (corresponding to a current density 0.9–1.5 A cm^{-2}), the electroluminescence spectrum was obtained. A weak blue shift and slightly larger width were obtained compared to the photolu-
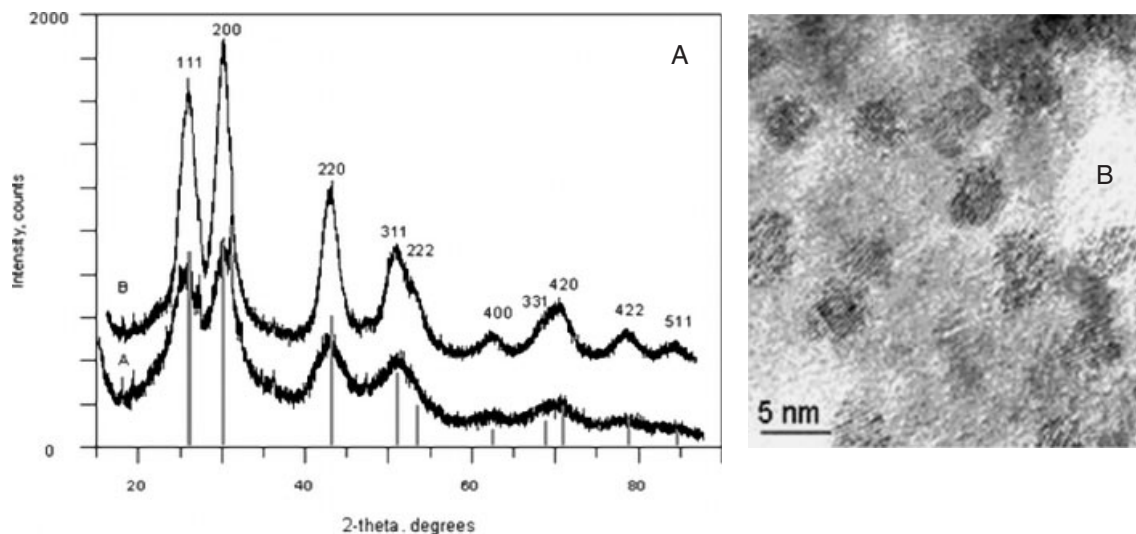
Figure 3. A) XRD patterns of PbS NCs: 1 h (bottom) and 14 days (top) after nanoparticle synthesis. B) High-resolution TEM image of PbS nanoparticles. Molar ratio of Pb/TGL/DTG was 1:6:2; Pb/S molar ratio was 1:0.5.
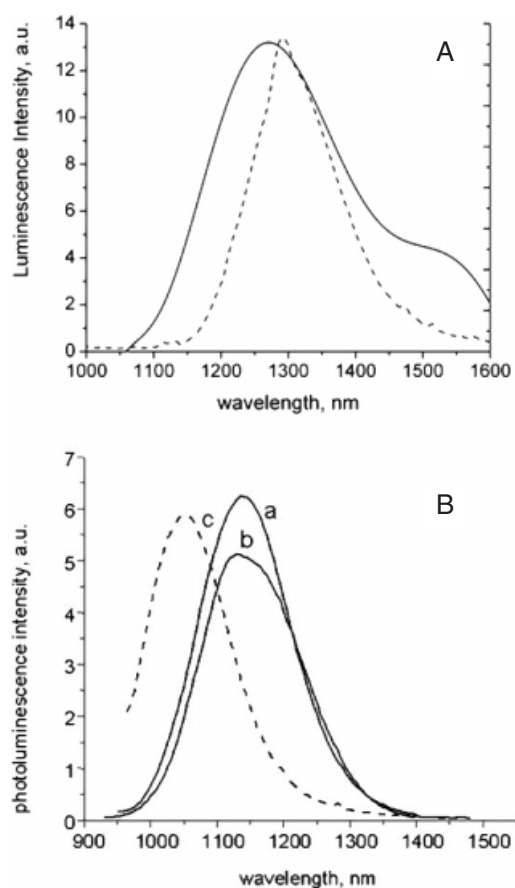
Figure 4. A) Photoluminescence (dashed curve) and electroluminescence (solid curve) spectra of a nanocomposite obtained by embedding PbS NCs into poly(p-phenylenevinylene) matrix. B) Photoluminescence spectra of identical PbS nanocrystals in DNA solution (a) and OVA protein (b). For comparison, the dashed line (c) shows the spectrum for nanocrystals of different size in OVA protein.

minescence spectrum. A similar difference between the photo- and electroluminescence spectra has been observed for water-soluble CdTe NCs.[24] In photoluminescence, electrons and holes are created in equal numbers directly inside NCs, while in electroluminescence, differences in transport of the two carrier types may result in charging of NCs, distortion of their band diagrams,[25] and the shift of effective bandgap in the presence of a local electric field.

With an eye to applications in fluorescent labeling, we measured photoluminescence of the NCs in solutions of biopolymers. Here, our focus was on retaining a narrow and intense stable luminescence that lies between the bands of strong absorption by water ($\lambda > 1200$ nm) and fluorescent background of biomolecules, typically in the visible spectrum (e.g., at $\lambda < 700$ nm for haemoglobin).[26] PbS NCs were dissolved in a) DNA solution and b) OVA protein (ovalbumin, a glycoprotein with molecular weight of 45 kDa) solution and cast on a quartz substrate. As before, changing NC size resulted in size-tunable photoluminescence (Fig. 4B). Measurements acquired over a 10 day period resulted in the same spectra and amplitude of luminescence in all environments.

In summary, the quantum dots reported herein combine efficient, stable, spectrally tunable luminescence from 1000 to 1400 nm, and facile one-stage aqueous synthesis. The fluorescent tags have a high quantum yield of photoluminescence and efficiencies that are largely independent of the environment, such as water, DNA, and OVA protein solutions, and when embedded in semiconducting polymer films. In the latter case, their short ligands enable efficient energy transfer from an electrically pumped semiconducting polymer matrix into the light-emitting quantum dots. These materials represent a new, simple, and scalable route to diverse applications in biological labeling and integrated optical fiber communications circuits.

Experimental

All chemicals were obtained from Sigma–Aldrich and used as received. The water used in all experiments had resistivity 18.2 MΩ cm.

Absorption spectra were recorded using a Cary 500 UV-vis-NIR spectrophotometer. Fluorescence spectra were measured using a PTI spectrometer with Ge liquid nitrogen-cooled detector. Luminescence excitation was provided by a laser at 831 nm. Absolute measurements of photoluminescence were carried in an integrating sphere at excitation from a semiconductor laser at wavelength of 831 nm, as described in reference [19]. The laser and photoluminescence spectra were measured for the incident light beam on the sample or on the wall of the integrating sphere.

TEM measurements were performed on a JEOL-2010-FEG microscope operated at 200 kV. TEM specimens were prepared by depositing a droplet of diluted PbS NCs solution onto carbon-coated copper grid and gently wicking away the excess.

A fully automated Siemens D5000 Diffractometer System was used for data collection in X-ray diffraction (XRD) experiments. The system was operating with Cu Kα fine focus target set up at 50 kV/35 mA. The secondary beam was monochromatized by a Kevex SS Detector. A step scan mode was used for data collection with step size: 0.02° 2θ and counting time of 6.0 s per step. The scanning range was 16–87°. A sample for XRD analysis was prepared by drying 20 mL of PbS NC aqueous solution under vacuum at room temperature.

The electroluminescent devices consisted of a glass substrate with an indium tin oxide anode contact cleaned by the argon plasma treatment; a 50 nm thick layer of water-based poly(p-phenylene vinylene) (PPV) polymer deposited by spin-coating; a 70–100 nm thick layer of nanocrystals added by spraying a nanocrystal-containing solution onto the polymer layer and an upper Mg cathode contact (200 nm) fabricated by vacuum evaporation with protection from the ambient atmosphere achieved with a 20 nm thick gold film.

[1] a) W. U. Huynh, J. J. Dittmer, A. P. Alivisatos, *Science* **2002**, *295*, 2425. b) V. I. Klimov, A. A. Mikhailovsky, Su Xu, A. Malko, J. A. Hollingsworth, C. A. Leatherdale, H.-J. Eisler, M. G. Bawendi, *Science* **2000**, *290*, 314. c) J. Joo, H. B. Na, T. Yu, J. H. Yu, Y. W. Kim, F. Wu, J. Z. Zhang, T. Hyeon, *J. Am. Chem. Soc.* **2003**, *125*, 11 100.

[2] a) V. S. Gurin, *J. Cryst. Growth* **1998**, *191*, 161. b) Z. H. Zeng, S. H. Wang, S. H. Yang, *Chem. Mater.* **1999**, *11*, 3365. c) Y. Jiang, Y. Wu, B. Xie, S. W. Yuan, X. M. Liu, Y. T. Qian, *J. Cryst. Growth* **2001**, *231*, 248.

[3] a) L. Bakueva, S. Musikhin, M. A. Hines, T.-W. F. Chang, M. Tzolov, G. D. Scholes, E. H. Sargent, *Appl. Phys. Lett.* **2003**, *82*, 2895. b) T. Ding, J. R. Zhang, S. Long, J. J. Zhu, *Microelectron. Eng.* **2003**, *66*, 46. c) S. H. Liu, X. F. Qian, J. Yin, H. W. Lu, Z. K. Zhu, *Mater. Sci. Eng. B* **2003**, *100*, 314.

[4] L. Bakueva, S. Musikhin, E. H. Sargent, H. E. Ruda, A. Shik, *Handbook of Organic — Inorganic Hybrid Materials and Nanocomposites* (Ed: H. S. Nalwa), American Scientific Publishers, Stevenson Ranch, CA **2003**.

[5] a) W. C. W. Chan, S. Nie, *Science* **1998**, *281*, 2016. b) M. Han, X. Gao, J. Z. Su, S. Nie, *Nat. Biotechnol.* **2001**, *19*, 631.

[6] M. T. Harrison, S. V. Kershaw, A. L. Rogach, A. Kornowski, A. Eychmüller, H. Weller, *Adv. Mater.* **2000**, *12*, 123.

[7] A. L. Rogach, M. T. Harrison, S. V. Kershaw, A. Kornowski, M. G. Burt, A. Eychmuller, H. Weller, *Phys. Status Solidi B* **2001**, *224*, 153.

[8] Jr., M. Bruchez, M. Moronne, P. Gin, S. Weiss, A. P. Alivisatos, *Science* **1998**, *281*, 2013.

[9] The ingredients used in synthesis of PbS NCs were less toxic than those used in synthesis of nanoparticles providing photoluminescence in the same spectral range (see, e.g., [16] for CdHgTe quantum dots).

[10] R. J. Lewis, *Sax's Dangerous Properties of Industrial Materials*, Vol. 1–3, Van Nostrand Reinhold, New York **1996**.

[11] A. L. Rogach, A. Eychmuller, J. Rockenberger, A. Kornowski, H. Weller, L. Troger, M. Y. Gao, M. T. Harrison, S. V. Kershaw, M. G. Burt, *Mater. Res. Soc. Symp. Proc.* **1999**, *536*, 365.

[12] A. Rogach, S. V. Kershaw, M. Burt, M. T. Harrison, A. Kornowski, A. Eychmüller, H. Weller, *Adv. Mater.* **1999**, *11*, 552.

[13] A. A. Patel, F. Wu, J. Z. Zhang, C. L. Torres-Martinez, R. K. Mehra, Yi Yang, S. H. Risbud, *J. Phys. Chem. B* **2000**, *104*, 11 598.

[14] D. Kim, N. Teratani, H. Nishimura, M. Nakayama, *Int. J. Mod. Phys. B* **2001**, *15*, 3829.

[15] The solution of TGL-stabilized NCs was also stored at 0 °C and removed from the ice bath prior to testing of NC stability under ambient conditions, optical characterization or further technological operations.

[16] a) A. L. Rogach, M. T. Harrison, S. V. Kershaw, A. Kornowski, M. G. Burt, A. Eychmuller, H. Weller, *Phys. Status Solidi B* **2001**, *224*, 153. b) A. L. Rogach, N. A. Kotov, D. S. Koktysh, A. S. Susha, F. Caruso, *Colloids Surf. A* **2002**, *202*, 135. c) M. T. Harrison, S. V. Kershaw, M. G. Burt, A. Rogach, A. Eychmuller, H. Weller, *J. Mater. Chem.* **1999**, *9*, 2721.

[17] C. B. Murray, D. J. Norris, M. G. Bawendi, *J. Am. Chem. Soc.* **1993**, *115*, 8706.

[18] R. S. Kane, R. E. Cohen, R. Silbey, *J. Phys. Chem.* **1996**, *100*, 7928.

[19] J. C. de Mello, H. F. Wittmann, R. H. Friend, *Adv. Mater.* **1997**, *9*, 230.

[20] A. L. Rogach, A. Kornowski, M. Gao, A. Eychmueller, H. Weller, *J. Phys. Chem. B* **1999**, *103*, 3065.

[21] Bruker AXS (2000): Topas V.2.1: General profile and structure analysis software for powder diffraction data (Users manual, Bruker AXS, Karlsruhe, Germany).

[22] Here, PbS NCs were used without purification by dialysis.

[23] B. O. Dabbousi, M. G. Bawendi, O. Onitsuka, M. F. Rubner, *Appl. Phys. Lett.* **1995**, *66*, 1316.

[24] N. P. Gaponik, D. V. Talapin, A. L. Rogach, *Phys. Chem. Chem. Phys.* **1999**, *1*, 1787.

[25] a) A. Shik, H. Ruda, E. H. Sargent, *J. Appl. Phys.* **2000**, *88*, 3448. b) A. Shik, S. Yu, E. Johnson, H. Ruda, E. H. Sargent, *Solid State Electron.* **2002**, *46*, 61.

[26] W. G. Zijlstra, *Visible and Near-Infrared Absorption Spectra of Human and Animal Haemoglobin*, VSP International Science Publishers, Boston, MA **2000**.

A Two-Stage Route to Coaxial Cubic-Aluminum-Nitride–Boron-Nitride Composite Nanotubes

By *Long-Wei Yin,* Yoshio Bando, Ying-Chun Zhu, Dmitri Golberg*, and *Mu-Sen Li*

Aluminum nitride, an important member of the group III nitrides with a bandgap of about 6.2 eV, is an attractive material for electronic substrates or for packaging, high-tempera-

[*] L.-W. Yin, Y. Bando, Y.-C. Zhu, D. Golberg
Advanced Materials Laboratory
National Institute for Materials Science
Namiki 1-1, Tsukuba, Ibaraki 305-0044 (Japan)
E-mail: YIN.Longwei@nims.go.jp
L.-W. Yin, M.-S. Li
College of Materials Science and Engineering, Shandong University
Jinan 250061 (P.R. China)